Inhibitor of differentiation 1 in U87MG glioblastoma cells promotes HUVEC sprouting through endothelin-1

SANG-HUN CHOI, MIN JI PARK and HYUNGGEE KIM

Department of Biotechnology, College of Life Science and Biotechnology, Korea University, Seoul 02841, Republic of Korea

Received July 16, 2022; Accepted September 6, 2022

DOI: 10.3892/ol.2022.13533

Abstract. Anti-angiogenesis therapy, a promising remedy against tumor progression, is now widely used to treat numerous types of cancer. Since vascular endothelial growth factor (VEGF) is the most vital factor in angiogenesis, most anti-angiogenesis drugs target the VEGF-related pathway. However, in glioblastoma (GBM), the therapeutic strategy involving the inhibition of VEGF signaling is ineffective. The present study demonstrated that the potential angiogenic function of endothelin-1 (EDN1) was upregulated by inhibitor of differentiation 1 (ID1) independent of VEGF during tumor angiogenesis. Anatomic structure transcriptomes of patients with GBM revealed that the expression levels of ID1 and EDN1 were specifically upregulated in the vascular-related region. The aortic ring assay and endothelial sprouting assay demonstrated that EDN1 more potently promoted endothelial sprouting ability than VEGF. The activity of EDN1 was induced by endothelin receptor, which seemed to mediate regulation via positive feedback. Finally, in patients with GBM who did not respond to bevacizumab, a VEGF antagonist, EDN1 expression was higher than that in bevacizumab responders. Collectively, the present study demonstrated that EDN1 is a potent angiogenic factor inducing endothelial sprouting and may be a novel target for inhibiting glioma angiogenesis.

Introduction

Blood vessels are essential elements for supplying oxygen and nutrients to maintain normal tissues (1). Angiogenesis, a process in which new blood vessels are developed, begins in embryogenesis. In adulthood, the process maintains a static state, except in certain conditions, such as inflammatory diseases. Vascular endothelial growth factor (VEGF) is a crucial component involved in promoting angiogenesis and can initiate angiogenesis by binding to VEGF receptor 2 (VEGFR2) in the endothelial cells (ECs) (2). The regulation of VEGFR2 by a positive feedback mechanism increases reliance on VEGF-induced angiogenesis. It can promote endothelial proliferation and sprouting (3).

The induction of angiogenesis in a static vascular state is termed 'angiogenic switch', which is one of the hallmarks of cancer (4,5). As the size of the tumor increases with cancer progression, the demand for blood vessels is indispensable. Hypoxia is a condition involving the absence of blood vessels observed during the typical progression of cancer. To overcome hypoxia and induce angiogenesis, cancer cells secrete VEGF, a pro-angiogenic factor. Hence, VEGF is a critical factor for cancer progression and growth (6).

The first anti-angiogenesis therapy involved administering the monoclonal antibody 'bevacizumab', which binds to the VEGFA isoform and interrupts the interaction between VEGFA and VEGFR. Bevacizumab was first approved by the FDA in 2004 for the treatment of metastatic colorectal cancer. it has since been used to treat various cancers, including breast cancer, non-small cell lung cancer, metastatic breast cancer, ovarian cancer, renal cell carcinoma, and recurrent glioblastoma (GBM) (7). Although bevacizumab has shown favorable outcomes in treating many cancers, no significant effect has been observed on GBM. Bevacizumab improves the quality of life but not the overall survival of patients with GBM (8). Induction of hypoxia via the inhibition of angiogenesis and VEGF-independent angiogenesis mechanisms has been reported. The precise reason remains primarily unknown.

Endothelin 1 (EDN1) was initially identified as a peptide hormone secreted from ECs and is known to act on smooth muscle cells (SMCs). Exposure of SMCs to EDN1 promotes vasoconstriction, and excessive EDN1 levels are a major factor contributing to the development of hypertension (9). At present, EDN1 functions in various types of cells, including cancer cells as well as in SMCs. In particular, it influences malignancy by increasing proliferation, suppressing apoptosis, and promoting the endothelial to mesenchymal transition (10). However, the effect of EDN1 on ECs and the relationship between ECs and cancer malignancy remain unknown.

According to a previous study conducted by our group, the inhibitor of differentiation 1 (ID1) may be associated with VEGF-independent angiogenesis in GBM. The growth

Correspondence to: Professor Hyunggee Kim, Department of Biotechnology, College of Life Science and Biotechnology, Korea University, 145 Anam-ro, Seongbuk-gu, Seoul 02841, Republic of Korea
E-mail: hg-kim@korea.ac.kr

Key words: inhibitor of differentiation 1, endothelin-1, glioblastoma, sprouting

rate increases in ID1-expressing GBM cells and promotes tumor angiogenesis (11). Therefore, we examined the association between ID1 and EDN1 and elucidated the angiogenic capability of EDN1.

Materials and methods

Cell culture and culture conditions. The human glioma cell line U87MG (*TP53*wt, *PTEN*mut, *p14ARF/p16*del) was purchased from the American Type Culture Collection (ATCC, Cat. HTB-14; glioblastoma of unknown origin). It was authenticated that the cell line was U87MG cells through short tandem repeat profiling. U87MG cells were cultured in Dulbecco's modified Eagle's medium-high glucose (DMEM; Lonza, Cat. SH30243.01) supplemented with 10% fetal bovine serum (FBS; Hyclone, Cat. SH30919.03), 1% penicillin/streptomycin (P/S; Hyclone, Cat. SV30010), and 2 mM L-glutamine (Cat. SH30034.01) at 37˚C in an atmosphere containing 5% CO_2 and 95% humidity.

Human umbilical vein endothelial cells (HUVECs) were purchased from Lonza (Lonza, Cat. CC-2517). HUVECs were cultured on 0.2% gelatin-coated plates (Sigma-Aldrich, Cat. G1890) and grown in an endothelial cell growth medium (EGM-2, Lonza, Cat. CC-3162). All experiments were conducted until passage five.

Plasmid construction and virus infection. U87MG cells were infected with lentivirus produced using the HEK293FT cell line (Life Technologies, Cat. R70007) that was transfected with a lentiviral vector (pLL-CMV-GFP, pLL-CMV-ID1-GFP) and packaging vectors (third-generation: pMDLg/pRRE, pRSV-Rev, and pMD2.G).

Western blot analysis. Western blotting was performed to analyze protein expression. Briefly, cell extracts were prepared using the RIPA lysis buffer (150 mM sodium chloride, 1% NP-40, 0.1% SDS, 50 mM Tris, pH 7.4) containing 1 mM β-glycerophosphate, 2.5 mM sodium pyrophosphate, 1 mM sodium fluoride, 1 mM sodium orthovanadate, and a protease inhibitor (Roche, Cat. 11836170001). The protein concentration was quantified using the Bradford assay reagent (Bio-Rad) according to the manufacturer's instructions. Proteins were resolved by SDS-PAGE and then transferred to a polyvinylidene fluoride membrane (Pall Corporation, Cat. BSP0861). The membranes were blocked with 5% non-fat milk and incubated with the following antibodies at indicated dilutions: anti-ID1 (1:1,000; Biocheck, Cat. BCH-1/195-14-50) and anti-β-actin (1:10,000; Santa Cruz Biotechnology, Cat. sc-47778). Membranes were then incubated with horseradish peroxidase-conjugated anti-IgG secondary antibody (Pierce Biotechnology) and visualized using the SuperSignal West Pico Chemiluminescent Substrate (Pierce Biotechnology, Cat. 34580).

Reverse transcription-quantitative PCR (RT-qPCR). RT-qPCR was performed to determine mRNA levels. Briefly, total RNA was isolated from cells using the QIAzol lysis reagent (QIAGEN, Cat. 79306) according to the manufacturer's instructions. Then, 1 U of DNase I (RNase-free; Thermo Fisher Scientific, Cat. EN0525) was added to 1 μg of template RNA, followed by incubation for 30 min at 37˚C. For inactivating DNase I, 50 mM of EDTA was added, followed by heating at 65˚C for 10 min. DNase I-treated RNA was used as a template for synthesizing complementary DNA (cDNA) using a RevertAid First Strand cDNA Synthesis Kit (Thermo Fisher Scientific, Cat. K1622) according to the manufacturer's instructions. RT-qPCR analysis was performed using Takara Bio SYBR Premix Ex Taq (Takara, Cat. RR420A) and CFX096 (Bio-Rad, Hercules, CA, USA) using the following thermocycling conditions: Initial denaturation at 95˚C for 30 sec, followed by 45 cycles at 95˚C for 5 sec and 60˚C for 30 sec for annealing and elongation. The expression of each target gene was *normalized* to that of *GAPDH* and quantified using the $2^{-\Delta\Delta Cq}$ method (12). The following primer sequences were used: human *GAPDH* forward: 5'-CTACACTGAGCA CCAGGTGGTCTC-3', reverse: 5'-GATGGATACATGACA AGGTGCGGC-3'; human *EDN1* forward: 5'-CGAGCACAT TGGTGACAGAC-3', reverse: 5'-GAAGATGGTTGGGGG AACTC-3'.

Transepithelial electrical resistance (TEER) value. To measure the TEER values of the monolayers, $5x10^4$ HUVECs were seeded into Transwell inserts (6.5 mm diameter, 5.0 μm pore size, Costar, Cat. 3421). Insert was pre-coated with fibronectin from human plasma (Sigma-Aldrich, Cat. F0895) in PBS for 2 h at 37˚C in an incubator and air-dried for 45 min. One hour after seeding the cells, the insert was transferred to an empty well containing 850 μl EGM-2 medium. The TEER value was measured one day after seeding using an ERS-2 epithelial volt-ohm meter (Millicell, Cat. MERS00002). The STX3 electrodes were introduced into the apical and basolateral compartments of the inserts. For each experiment, the TEER value was measured in a cell-free Transwell insert (blank). The final TEER values were multiplied by the surface area of the inserts and expressed as Ωcm^2.

Mouse aortic ring assay. Aortas obtained from two-week-old C57/BL/6J mice were cut into approximately 1.0 mm pieces, as previously described (13). Briefly, following a chest incision, the lungs and liver are removed, which reveals the aorta. Using forceps and scalpel, separate the aorta from the spine. The fibroadipose tissue around the aorta was carefully removed. Transfer the isolated aorta to an ice-cold culture dish containing EGM-2 medium. Using a scalpel, cut the aorta into 1.0 mm pieces. The aortic rings were cultured in 48-well Matrigel-coated plates (Corning, Cat. 354234). Next, 500 μl of EGM-2 medium containing VEGF (100 μg/ml; R&D Systems, Cat. 293-VE-050) and EDN1 (100 μg/ml; TOCRIS, Cat. 1160/100 U) was added to each well. After five days, the aortic rings were fixed with 4% PFA and images were captured by microscopy (Olympus, Cat. CKK53, magnification x10). The image analysis was performed by Image J (software v.1.52a, plugin; Angiogenesis Analyzer, http://imagej.nih.gov/ij/). The Korea University Institutional Animal Care & Use Committee approved the animal experiments, which were carried out in accordance with governmental and institutional guidelines as well as Korean regulations (approval no. KUIACUC-2019-0040). A total of 10 male C57/BL/6J mice (1 week old; average weight, 3 g) were purchased by Orient Bio, Inc. Mice were bred with

under conditions that included an average temperature of 20-24˚C, humidity of 45-65%, and a 12-h light/dark cycle. The mice were received a continuous supply of food and water. When the mice were 2 weeks old, they were anesthetized by inhalation of 30% CO_2 (4.5 l/min) for 2 min in a CO_2 gas chamber.

HUVEC spheroid sprouting assay. HUVECs ($1x10^3$) were mixed with a 0.25% methylcellulose solution (Sigma-Aldrich, Cat. M0512) and EBM-2 (Lonza, Cat. CC-3156). A total of 20 μl of the mixture containing 1,000 cells was dispensed using the hanging-drop method and incubated overnight at 37˚C in an atmosphere containing 5% Co_2 for spheroid formation. Next, 61 μl of collagen was added, and the total volume of the collagen mixture was 100 μl (4.07 mg/ml stock, Corning, Cat. 354236). The spheroids were gently washed off the hanging-drop plate with phosphate-buffered saline (PBS), centrifuged at 500 rpm using a swing bucket rotor for 5 min, and re-suspended in 60 μl of 0.25% methylcellulose solution. A total of 60 μl of 0.25% methylcellulose solution containing HUVEC spheroids was added to the aforementioned mixture. A total of 150 μl of the final mixture was dispensed into 48-well plates and polymerized at 37˚C in an incubator for 30 min. The appropriate wells were then overlaid with 500 μl of complete EGM-2 containing VEGF (100 μg/ml; R&D system, Cat. 293-VE-050) and EDN1 (100 μg/ml; TOCRIS, Cat. 1160/100U) recombinant protein. Endothelial sprouting was observed and fixed with 4% PFA for immunofluorescence (IF) analysis after five days. The image was analyzed by Image J (software v.1.52a, plugin; Angiogenesis Analyzer, Analyze Particles, http://image.nih.gov/ij/).

Preparation of conditioned medium (CM). For the collection of CM, U87MG-GFP, and U87MG-ID1-GFP cells ($7.5x10^5$) were seeded in a 100-mm culture plate with DMEM containing 10% FBS. After 48 h, the medium was replaced with an EGM-2 medium. After 24 h, the CM was harvested and filtered using 0.2-μm filters (Sartorius, Cat. 16534).

Fluorescence images. Fluorescence image analysis was performed as previously described (14). HUVEC spheroids were fixed in 4% PFA for 15 min at room temperature (RT). The spheroids were washed thrice with PBS, permeabilized with 0.3% Triton X-100 in PBS for 10 min at RT, and then blocked with 3% BSA (Merck, Cat. 82-100-6) in PBS for 1 h at RT. The spheroids were incubated with CD31 antibody (1:200, Thermo Fisher, Cat. IHC-00055), EDNRA antibody (1:200, Alomone Labs, Cat. AER-001), and EDNRB antibody (1:200, Alomone Labs, Cat. AER-002) overnight at 4˚C, followed by incubation with Alexa Fluor 488- or 568-conjugated secondary antibodies (1:400, ThermoFisher, Cat. A10042, A21202) for 2 h at RT. Nuclei were then stained with DAPI (1 μg/ml, Sigma-Aldrich, Cat. D9542) for 5 min. For phalloidin staining (Invitrogen, Cat. A12379), HUVECs were fixed in 4% PFA for 15 min at RT. They were washed thrice with PBS, permeabilized with 0.3% Triton X-100 (Sigma-Aldrich, Cat. T9281) in PBS for 10 min at RT, and then blocked with 3% BSA in PBS for 1 h at RT. The spheroids were incubated with phalloidin (6.6 μM) for 2 h at RT. Nuclei were then stained with DAPI for 5 min.

Fluorescence images were obtained using confocal laser scanning microscopy [LSM800; Carl Zeiss, ZEN acquisition software version 2018 (blue edition)] at RT (magnification x10).

In silico analysis. To analyze region-specific transcriptome profiles of patients with GBM, we obtained fragments per kilobase of transcripts per million mapped reads data from the Ivy glioblastoma atlas project (Ivy GAP) website (http://glioblastoma.alleninstitute.org/). Regional information was divided into seven types: hyperplastic blood vessels in the cellular tumor (n=22), microvascular proliferation (n=28), leading-edge (n=19), infiltrating tumor (n=24), cellular tumor (n=111), perinecrotic zone (n=26), and pseudopalisading cells around necrosis (n=40). The relative genes were converted to z-scores, and the mean ± SD value of the z-score was calculated.

The ID1 RNA-seq data obtained by eBiogen were grouped based on changes in the expression higher than two-fold of the baseline value to establish an ID1 signature determined by comparing the mean expression values (Student's t-test; $P<0.05$) (GEO: GSE182670).

To analyze the clinical relevance, we obtained transcriptome profiles of patients with GBM with or without bevacizumab treatment (15). Analyses were performed for all datasets with the exception of maximum and minimum values in bevacizumab responders and non-responders.

Statistical analysis. All statistical analysis was performed using an unpaired Student's t-test and one-way ANOVA test followed by Bonferroni post hoc test. When comparing two groups, the significance was determined using a student's t-test. Comparison between multiple groups was determined one-way ANOVA test followed by Bonferroni post hot test. All statistical analysis was performed using GraphPad Prism (Version 9.3.1). Values of $P<0.05$ or $P<0.01$ were considered statistically significant for different experiments, as indicated in figure legends. Data are presented as mean ± SEM.

Results

mRNA expression of ID1 and EDN1 is primarily observed in the vascular-related region in tissues of patients with GBM. To investigate the genes regulated by ID1 that affect ECs, we performed RNA sequencing using the ID1-overexpressing U87MG cell line. Next, we merged upregulated differentially expressed genes (DEGs) from RNA sequencing data (>two-fold, <FDR value 0.05, n=433) using a gene set (Module 92: secreted signaling molecules, n=149) to identify factors that can affect ECs. Three genes (*NMU*, *WISP2*, and *EDN1*) were selected (Fig. 1A). Subsequently, we used the Ivy GAP project (http://glioblastoma.alleninstitute.org/), which consists of the transcriptome data of seven anatomic structures isolated via laser microdissection from patients with GBM, to validate the genes that influence the synthesis of ECs among the three genes. Interestingly, only *ID1* and *EDN1* were highly expressed in the vascular-related region (microvascular proliferation and hyperplastic blood vessels). Particularly, *EDN1* was scarcely expressed, except in the vascular-related region (Fig. 1B and C). Collectively, we verified the possibility that *EDN1* could function in the ECs of patients with GBM.

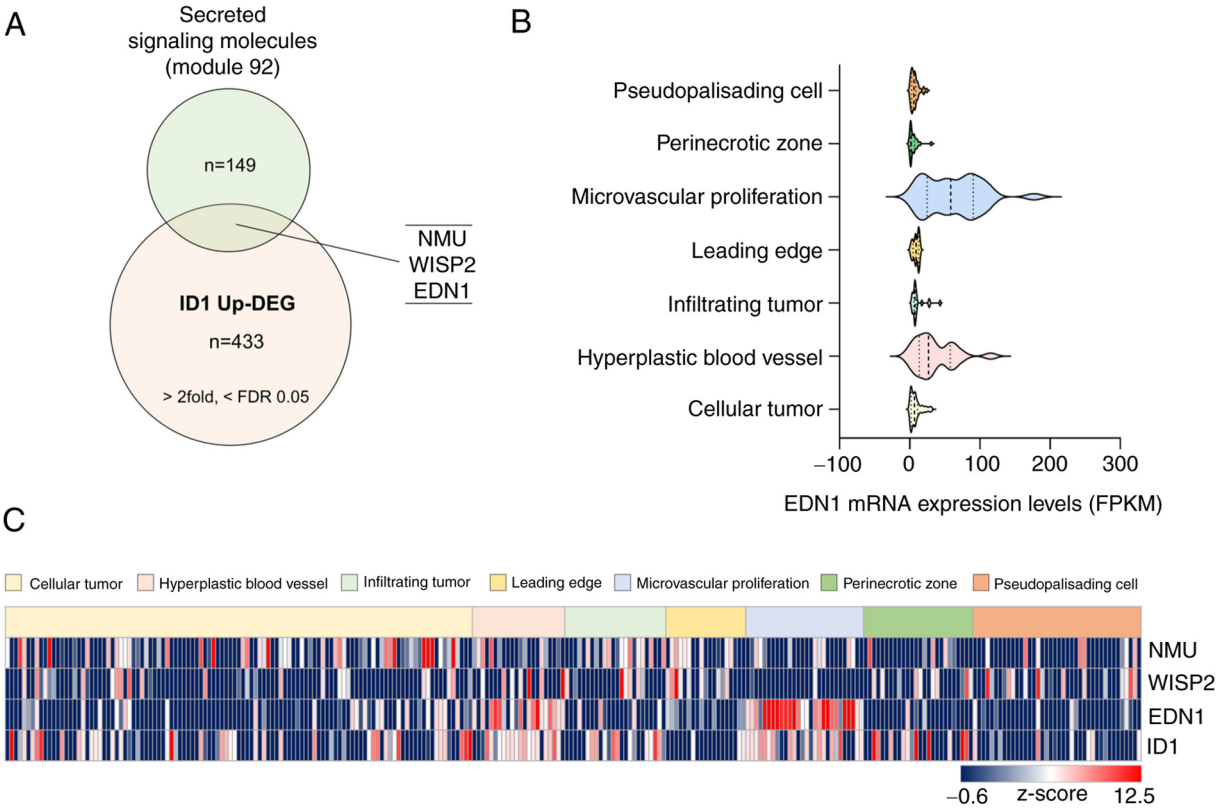

Figure 1. EDN1 expression, which is upregulated by ID1, is elevated in the vascular-related region in tissues derived from patients with GBM. (A) Venn diagram obtained after merging two datasets to identify vascular regulating factors associated with ID1 (Module 92 refers to a list containing 149 secreted signaling molecules in humans, n=149, https://www.gsea-msigdb.org/gsea/msigdb/cards/module_92; ID1 Up-DEG, n=433, >2 fold, <FDR value 0.05). (B) mRNA expression levels of EDN1 in tissues of patients with GBM were determined using the Ivy GAP database. (C) Identification of mRNA expression of candidate genes (*NMU*, *WISP*, *EDN1* and *ID1*) using the Ivy GAP database (http://glioblastoma.alleninstitute.org/). The relative mRNA levels were converted to z-score and are presented using a heat-map. EDN1, endothelin1; FDR, false discovery rate; FPKM, fragments per kilobase of exon per million mapped fragments; GBM, glioblastoma; ID1, inhibitor of differentiation 1; ID1 Up-DEG, ID1 Upregulated-Differentially Expressed Genes; Ivy GAP, Ivy glioblastoma atlas project; NMU, neuromedin u; WISP2, wnt1 inducible signaling pathway protein 2.

EDN1 promotes endothelial sprouting ability. We investigated whether the expression of *EDN1* was upregulated after *ID1* overexpression in U87MG cells. The mRNA expression of EDN1 was increased by six-fold in U87MG cells with ID1 overexpression compared to that in control cells (Fig. 2A). Next, we analyzed the maintenance of barrier function and sprouting ability, which are basic properties of ECs that could be influenced by EDN1. First, we observed no changes in the barrier function when HUVECs were treated with EDN1 (Fig. 2B). Second, we performed *ex-vivo* culture using mouse arteries to analyze the sprouting ability. Upon treatment with EDN1, the sprouting ability was predominantly promoted compared to that in the control and VEGF-treated groups (Fig. 2C). EDN1 is a more potent pro-angiogenic factor than VEGF. The tendency of EDN1 to increase the sprouting ability of ECs was also observed in the HUVEC spheroid sprouting model (Fig. 2D). When EDN1 was added, the sprouting length and sprouting cell number increased. Consequently, EDN1 did not affect the barrier function but increased sprouting ability, which is critical in the early stages of angiogenesis.

Putative positive feedback of EDNRB modulates endothelial sprouting. Endothelial culture media contains various growth factors. Therefore, the determination of the function of specific factors is limited. To overcome this limitation, we compared the endothelial sprouting ability induced by VEGF and EDN1 in basal media without growth factors. Results showed that EDN1 induced superior endothelial sprouting compared to VEGF, and no synergistic effect was observed between the two factors (Fig. 3A). EDN1 signaling is regulated by two receptors, EDNRA and EDNRB, and each receptor functions depending on the location of the tissue. We used bosentan, which can inhibit both EDN receptors, to determine whether EDNR regulated the increase in the EDN1-mediated sprouting in ECs. EDN1 and bosentan combinedly demonstrated a sprouting tendency similar to that of the control group (Fig. 3B). This finding implies that the EDN1-EDNR axis promoted the sprouting ability of HUVECs. VEGF, a representative angiogenic factor, induces angiogenesis upon binding to VEGFR2. In this process, VEGFR2 maintains and amplifies VEGF signaling via positive feedback in tip cells rather than in stalk cells. To determine whether this phenomenon could also be attributed to EDNR, we compared EDNR expression after treatment with EDN1. Notably, the EDNR expression was extremely low when the cells were not treated with EDN1. However, EDNRB expression increased in the presence of EDN1 (Fig. 3C). In addition, EDNRB expression was primarily observed in the tip cells. Hence EDN1 induced endothelial sprouting by binding to EDNRB, and EDNRB may be regulated by positive feedback.

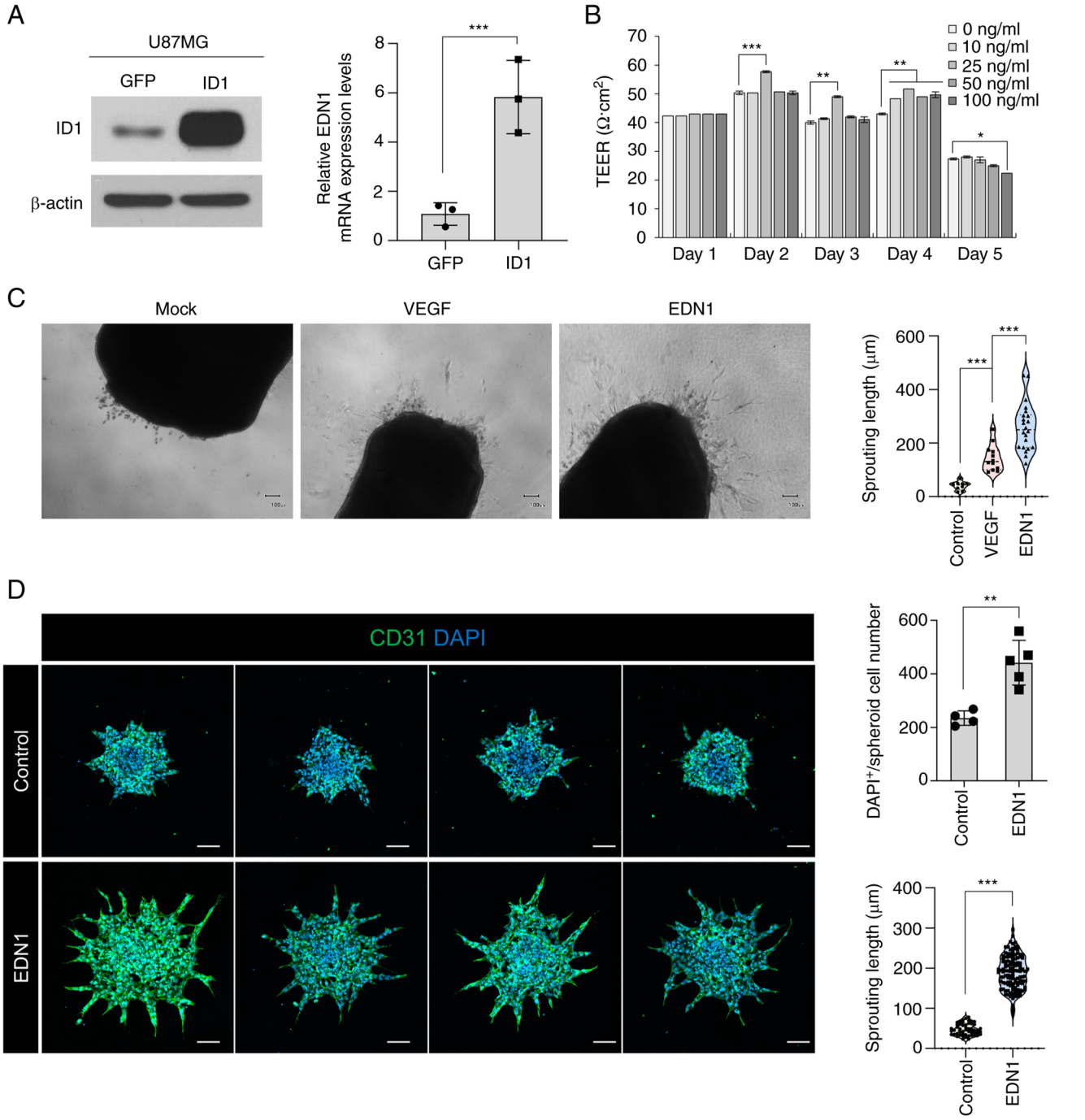

Figure 2. EDN1 induces endothelial sprouting. (A) ID1 and β-actin protein levels in ID1 overexpressing U87MG cells. EDN1 mRNA levels in ID1 overexpressing U87MG cells were determined using reverse transcription-quantitative PCR. ***P<0.001. Data are presented as the mean ± SEM. (B) TEER value of HUVECs after treatment with EDN1. *P<0.05; **P<0.01; ***P<0.001. Data are presented as the mean ± SEM. (C) Mouse aorta samples were cultured in the presence or absence of VEGF (100 ng/ml) and EDN1 (100 μg/ml) for 5 days. Quantification of the sprouting length in mouse aortas. ***P<0.001. Data are presented as the mean ± SEM. Scale bar, 100 μm. (D) HUVEC spheroids were cultured in the presence or absence of EDN1 (100 μg/ml; green, CD31; blue, DAPI). Quantification of the DAPI⁺ cell number and the sprouting length in HUVEC spheroids. **P<0.01; ***P<0.001. Data are presented as the mean ± SEM. Scale bar, 100 μm. EDN1, endothelin1; ID1, inhibitor of differentiation 1; TEER, transepithelial electric resistance; VEGF, vascular endothelial growth factor; GFP, green fluorescent protein.

Promotion of endothelial sprouting by the ID1-EDN1-EDNRB axis and its clinical relevance. To confirm the association between ID1 and EDN1, we used a CM collected from glioblastoma cells that overexpressed ID1 (ID1_CM) and those that did not demonstrate overexpression (GFP_CM). The CM was obtained using the EGM-2 medium, which was used for the HUVEC spheroid sprouting assay (Fig. 4A). Upon confirming the expression of EDN1 when obtaining CM, we observed that the number of cells overexpressing ID1 was approximately 40 times higher than that of the control cells (Fig. 4B). However, sprouting was not observable on the spheroid when only CM was treated because of lack of basic nutrients (data not shown). So the CM was mixed with fresh EGM-2 medium in half and treated every day. When treated with ID1_CM, the sprouting ability

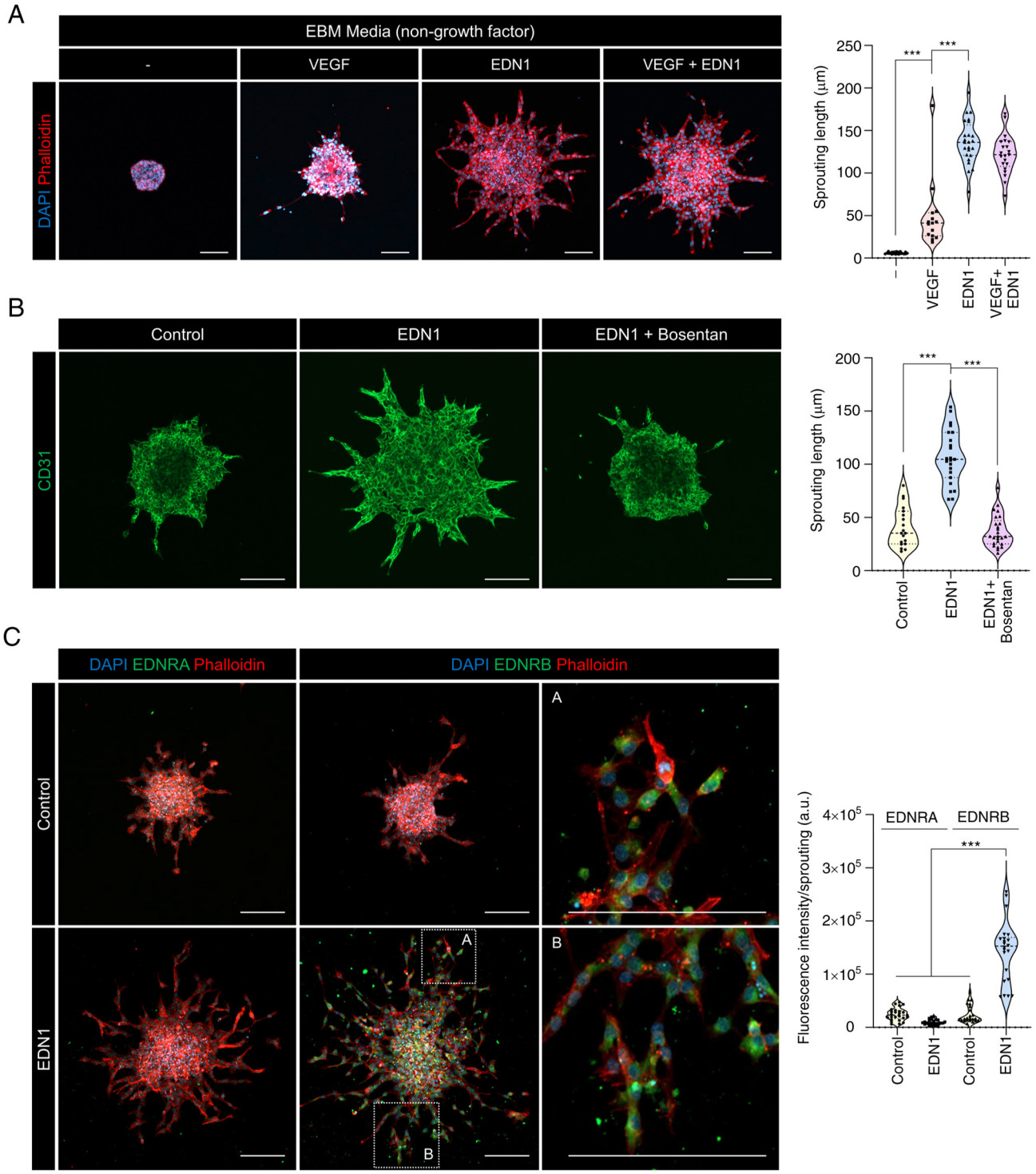

Figure 3. EDN1-EDNRB axis promotes endothelial sprouting, and its pro-angiogenesis function is more potent than that of VEGF. (A) HUVEC spheroids were cultured in the presence or absence of VEGF (50 ng/ml) and EDN1 (50 ng/ml) in EBM basal medium (red, phalloidin; blue, DAPI). Quantification of the sprouting length in HUVEC spheroids. ***P<0.001. Data are presented as the mean ± SEM. Scale bar, 100 μm. (B) HUVEC spheroids were cultured in the presence or absence of EDN1 (100 ng/ml) and bosentan (10 μM) (green, CD31). Quantification of the sprouting length in HUVEC spheroids. ***P<0.001. Data are presented as the mean ± SEM. Scale bar, 100 μm. (C) HUVEC spheroids were cultured in the presence or absence of EDN1 (100 ng/ml; green, EDNRA and EDNRB; red, phalloidin; blue, DAPI). Quantification of the fluorescence intensity (EDNRA and EDNRB) in the sprouting region. ***P<0.001. Data are presented as the mean ± SEM. Scale bar, 100 μm. EDN1, endothelin1; EDNRA, endothelin receptor type a; EDNRB, endothelin receptor type b; VEGF, vascular endothelial growth factor.

was higher than that observed with GFP_CM (Fig. 4C). Next, we used bosentan to determine whether sprouting was increased by EDN1 in ID1_CM. The increase in sprouting by ID1_CM was inhibited by bosentan (Fig. 4D). This result suggests that the EDN1 in ID1_CM induced sprouting. Finally, to assess the clinical relevance of EDN1, we compared the transcriptomes of bevacizumab-responders and non-responders in the cohort of patients with GBM (14). Patients responsive to bevacizumab

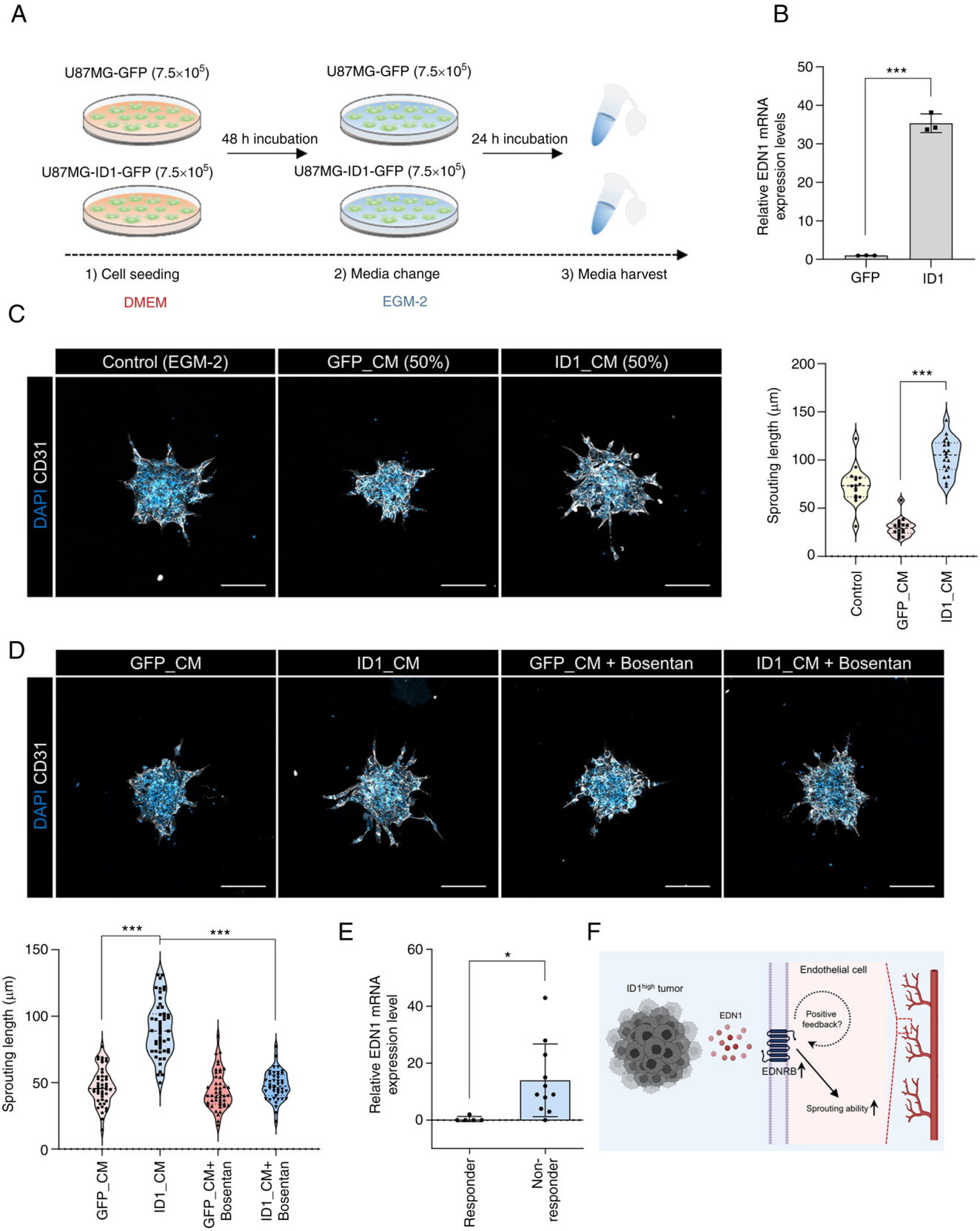

Figure 4. Relationship between ID1 and EDN1 and its clinical relevance. (A) A schematic diagram of the CM experiment. (B) mRNA expression levels of EDN1 in ID1 overexpressing U87MG cells were determined by reverse transcription-quantitative PCR using CM. ***P<0.001. Data are presented as the mean ± SEM. (C) HUVEC spheroids were cultured in the presence or absence of CM (white, CD31; blue, DAPI). Quantification of the sprouting length in HUVEC spheroids. ***P<0.001. Data are presented as the mean ± SEM. Scale bar, 100 μm. (D) HUVEC spheroids were cultured in the presence or absence of GFP_CM, ID1_CM and bosentan (10 μM) (white, CD31; blue, DAPI). Quantification of the sprouting length in HUVEC spheroids (bottom-left graph). ***P<0.001. Data are presented as the mean ± SEM. Scale bar, 100 μm. (E) mRNA expression levels of EDN1 in bevacizumab-responders or non-responders in the cohort of patients with GBM (responder, n=5; non-responder, n=11). *P<0.05. Data are presented as the mean ± SEM. (F) Graphical summary of the study (created with BioRender.com). CM, conditioned medium; EDN1, endothelin1; EDNRB, endothelin receptor type b; EGM-2, endothelial cell growth medium-2; GFP, green fluorescent protein; ID1, inhibitor of differentiation 1.

had low EDN1 expression, whereas non-responsive patients had higher EDN1 expression (Fig. 4E). This finding implies that EDN1, which is upregulated by ID1, can potentially be an angiogenic factor that can be targeted instead of VEGF during the treatment of patients with GBM (Fig. 4F).

Discussion

The role of blood vessels in cancer maintenance and progression has been recognized for a long time. Identifying factors that promote angiogenesis, a hallmark of cancer, serves as a foundation for anticancer strategies. VEGF, a master regulator of angiogenesis, has been identified, and bevacizumab has been developed to inhibit VEGF (1,4,5). However, unresponsiveness has been observed in patients decades after bevacizumab administration. The VEGF-independent angiogenesis pathway is a representative cause of resistance to anti-VEGF therapy (16). Therefore, identifying new pro-angiogenic factors is critical.

In this study, we demonstrated a novel pro-angiogenic, namely, EDN1. EDN1 increased sprouting ability at an early stage of angiogenesis and was more potent than VEGF. In addition, the EDNR demonstrated a positive feedback mechanism similar to that of VEGFR2, a characteristic of tip cells, which are known as sprouting cells in angiogenesis. To maintain a continuous VEGF signal, the tip cell induces lateral inhibition, suppressing VEGFR2 expression in the stalk cell, and VEGFR2 expression is sustained through the positive feedback of VEGFR2. Although the positive feedback mechanism of EDNRB mediated by EDN1 has not been precisely elucidated, such regulation via positive feedback might exist based on the fact that the expression of EDNRB is increased by the action of EDN1 in tip cells.

EDN1 is a vasoconstrictor peptide produced by endothelial cells. EDN1 induces vasoconstriction as a paracrine effect by acting on mural cells, such as pericytes and smooth muscle cells (9). Therefore, it contributes to the onset and progression of many hypertension-related diseases. Bosentan, which is capable of inhibiting EDNR, has also been developed (17). Consequently, the paracrine effect of EDN1 on mural cells has been well defined, but the paracrine effect on endothelial cells mediated by cancer cells is unknown. Most blood vessels in cancer are leaky. The primary cause of this phenomenon is the detachment of mural cells from endothelial cells (18). Kim *et al* (19) demonstrated that in a GBM mouse model, the coverage of pericytes surrounding the endothelial cells was reduced. Results showed that the expression of EDN1 was high in the vascular-related region in the Ivy GAP database. Collectively, the paracrine effect of EDN1 on endothelial cells from cancer cells may prevail over that on mural cells in cancer blood vessels. Although the paracrine effect of EDN1 on endothelial cells was not verified *in vivo*, it is planned to examine the effect in the future using a mouse model.

Results suggest that ID1 is an upstream factor for EDN1. However, the detailed mechanism underlying the regulation of EDN1 by ID1 has not yet been elucidated. ID1 has a helix-loop-helix structure and lacks a basic DNA-binding domain; therefore, it cannot independently bind to DNA. A well-known ID1 signaling mechanism forms a heterodimer with E protein, a basic helix-loop-helix structure, and suppresses cellular differentiation (20). Therefore, finding the binding partner of ID1 in the future is critical for understanding the ID1-EDN1 regulatory mechanism.

In summary, we suggest a target that can be used to develop treatment strategies for patients with GBM who are resistant to anti-angiogenic therapy, which is currently used to eradicate cancer.

Acknowledgements

Not applicable.

Funding

The present study was supported by grants from the National Research Foundation of Korea (NRF) (2020R1A2C2099668), College of Life Sciences and Biotechnology, Korea University (K2207511) and Brain Korea 21 PLUS.

Availability of data and materials

The datasets used and/or analyzed during the current study are available from the corresponding author on reasonable request. The RNA-seq data generated and/or analyzed during the current study are available in the GEO repository, https://www.ncbi.nlm.nih.gov/geo/query/acc.cgi?acc=GSE182670.

Authors' contributions

SHC, MJP and HK designed the experiments and wrote the manuscript. SHC conducted most experiments and analyzed the data. MJP performed molecular experiments. This study was directed by HK. All authors read and approved the final manuscript. SHC, MJP and HK confirm the authenticity of the raw data.

Ethics approval and consent to participate

Animal experiments were performed in the specific-pathogen-free facility with the approval of the Korea University Institutional Animal Care & Use Committee (approval no. KUIACUC-2019-0040; Seoul, Republic of Korea) and according to the governmental and institutional guidelines and Korean regulations.

Patient consent for publication

Not applicable.

Competing interests

The authors declare that they have no competing interests.

References

1. Adams RH and Alitalo K: Molecular regulation of angiogenesis and lymphangiogenesis. Nat Rev Mol Cell Biol 8: 464-478, 2007.
2. Shibuya M: Vascular endothelial growth factor (VEGF) and its receptor (VEGFR) signaling in angiogenesis: A crucial target for anti- and pro-angiogenic therapies. Genes Cancer 2: 1097-1105, 2011.

3. Page DJ, Thuret R, Venkatraman L, Takahashi T, Bentley K and Herbert SP: Positive feedback defines the timing, magnitude, and robustness of angiogenesis. Cell Rep 27: 3139-3151.e5, 2019.
4. Bergers G and Benjamin LE: Tumorigenesis and the angiogenic switch. Nat Rev Cancer 3: 401-410, 2003.
5. Hanahan D and Weinberg RA: Hallmarks of cancer: The next generation. Cell 144: 646-674, 2011.
6. De Bock K, Mazzone M and Carmeliet P: Antiangiogenic therapy, hypoxia, and metastasis: Risky liaisons, or not? Nat Rev Clin Oncol 8: 393-404, 2011.
7. Garcia J, Hurwitz HI, Sandler AB, Miles D, Coleman RL, Deurloo R and Chinot OL: Bevacizumab (Avastin®) in cancer treatment: A review of 15 years of clinical experience and future outlook. Cancer Treat Rev 86: 102017, 2020.
8. Gramatzki D, Roth P, Rushing EJ, Weller J, Andratschke N, Hofer S, Korol D, Regli L, Pangalu A, Pless M, *et al*: Bevacizumab may improve quality of life, but not overall survival in glioblastoma: An epidemiological study. Ann Oncol 29: 1431-1436, 2018.
9. Dhaun N and Webb DJ: Endothelins in cardiovascular biology and therapeutics. Nat Rev Cardiol 16: 491-502, 2019.
10. Rosanò L, Spinella F and Bagnato A: Endothelin 1 in cancer: Biological implications and therapeutic opportunities. Nat Rev Cancer 13: 637-651, 2013.
11. Jin X, Jeon HM, Jin X, Kim EJ, Yin J, Jeon HY, Sohn YW, Oh SY, Kim JK, Kim SH, *et al*: The ID1-CULLIN3 axis regulates intracellular SHH and WNT signaling in glioblastoma stem cells. Cell Rep 16: 1629-1641, 2016.
12. Livak KJ and Schmittgen TD: Analysis of relative gene expression data using real-time quantitative PCR and the 2(-Delta Delta C(T)) method. Methods 25: 402-408, 2001.
13. Park MH, Kim AK, Manandhar S, Oh SY, Jang GH, Kang L, Lee DW, Hyeon DY, Lee SH, Lee HE, *et al*: CCN1 interlinks integrin and hippo pathway to autoregulate tip cell activity. Elife 8: e46012, 2019.
14. Lee SY, Choi SH, Lee MS, Kurmashev A, Lee HN, Ko YG, Lee K, Jeong S, Seong J, Kang JH and Kim H: Retraction fibers produced by fibronectin-integrin α5β1 interaction promote motility of brain tumor cells. FASEB J 35: e21906, 2021.
15. Urup T, Staunstrup LM, Michaelsen SR, Vitting-Seerup K, Bennedbæk M, Toft A, Olsen LR, Jønson L, Issazadeh-Navikas S, Broholm H, *et al*: Transcriptional changes induced by bevacizumab combination therapy in responding and non-responding recurrent glioblastoma patients. BMC Cancer 17: 278, 2017.
16. Ferrara N: Pathways mediating VEGF-independent tumor angiogenesis. Cytokine Growth Factor Rev 21: 21-26, 2010.
17. Gabbay E, Fraser J and McNeil K: Review of bosentan in the management of pulmonary arterial hypertension. Vasc Health Risk Manag 3: 887-900, 2007.
18. Lugano R, Ramachandran M and Dimberg A: Tumor angiogenesis: Causes, consequences, challenges and opportunities. Cell Mol Life Sci 77: 1745-1770, 2020.
19. Kim IK, Kim K, Lee E, Oh DS, Park CS, Park S, Yang JM, Kim JH, Kim HS, Shima DT, *et al*: Sox7 promotes high-grade glioma by increasing VEGFR2-mediated vascular abnormality. J Exp Med 215: 963-983, 2018.
20. Lasorella A, Benezra R and Iavarone A: The ID proteins: Master regulators of cancer stem cells and tumour aggressiveness. Nat Rev Cancer 14: 77-91, 2014.